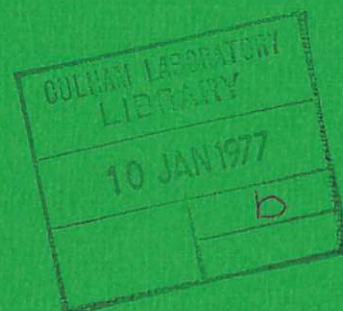




UKAEA

Preprint



THE CONSTRUCTION AND PERFORMANCE OF A 20 PPS UNSTABLE Nd:YAG OSCILLATOR

D ANDREOU

CULHAM LABORATORY
Abingdon Oxfordshire

1977

This document is intended for publication in a journal or at a conference and is made available on the understanding that extracts or references will not be published prior to publication of the original, without the consent of the authors.

Enquiries about copyright and reproduction should be addressed to the Librarian, UKAEA, Culham Laboratory, Abingdon, Oxfordshire, England

THE CONSTRUCTION AND PERFORMANCE OF A 20 PPS UNSTABLE Nd:YAG OSCILLATOR

D. Andreou*

UKAEA Culham Laboratory, Abingdon, Oxfordshire, OX14 3DB, UK.

ABSTRACT

A positive branch Nd:YAG unstable oscillator using a small reflecting spot centred on anti-reflection coated substrate as the output mirror has been constructed. The confocal condition is achieved by taking account of the lensing effect of the rod as well as the back mirror curvature. Q-switched output energies of 180 mJ in 10 ns have been obtained in a diffraction limited beam with a divergence of less than 0.25 mrad, at an overall efficiency of 1.3%.

* On attachment from Royal Holloway College, University of London, Englefield Green, Surrey.

(Submitted for publication in Review of Scientific Instruments)

October 1977.

THE CONSTRUCTION AND PERFORMANCE OF A 20 PPS
UNSTABLE Nd:YAG OSCILLATOR

D. Andreou *

UKAEA Culham Laboratory, Abingdon, Oxon, OX14 3DB.

INTRODUCTION

The construction of Nd:YAG unstable oscillators has recently become of growing importance due mainly to the high energies which can be obtained in a uniphase output. A negative branch Nd:YAG unstable oscillator has been reported.⁽¹⁾ This kind of oscillator however can deliver only limited amounts of energy due to the breakdown that occurs at the focal point inside the cavity. Its applications are therefore limited to low energy requirement systems such as rangefinders. A 10 pps positive branch Nd:YAG unstable oscillator has recently been reported by Herbst et al,⁽²⁾ which was used to drive nonlinear crystals. This has indicated the wide range of applications of the Nd:YAG unstable resonator, and the construction of high repetition rate systems has become of great importance.

In this paper the design, construction and performance of a 20 pps Nd:YAG unstable oscillator are described. New features include the construction of the output mirror and the calculation of the confocal condition, the latter being very

* On attachment from Royal Holloway College, University of London, Englefield Green, Surrey.

important in high repetition rate systems due to the strong lens formed in the laser rod. The quality of the output beam was investigated with a scanning diode array in the near and far fields. Q-switched output energies of 180 mJ in 10 ns have been obtained in a diffraction limited beam with a divergence of less than 0.25 mrad, and an overall efficiency of 1.3%.

DESIGN AND CONSTRUCTION

A commercially available Nd:YAG system - model 2000 from J.K. Lasers - was used in the experiments. The oscillator head contained a 3"x $\frac{1}{4}$ " rod pumped by a linear flashlamp and cooled with a recirculated liquid. One of the main problems in the operation of high repetition rate Nd:YAG lasers is the establishment of a thermal lensing effect in the laser rod. This greatly influences the confocal condition in a positive branch unstable resonator. In order to measure the focal length of the laser rod, a He-Ne laser was beam expanded to fill its diameter with a collimated beam, and the flashlamp was fired at different repetition rates. The focal length of the rod was thus measured for different pumping powers to the flashlamp at the He-Ne wavelength and then corrected to the neodymium wavelength. Fig.1 shows a plot of the focal length of the rod against the inverse of the input power to the flashlamp. The focal length of the rod can be approximated very closely to $f(m) = \frac{1.25}{P(kW)}$. The latter relation gives a much longer focal length for our oscillator rod than that reported in (2) for the same input power. It was thus easier to operate the system at higher repetition rates without serious distortion effects which might occur in the beam due to strong focusing in the rod.

The oscillator cavity was designed using the canonical formulation described by Siegman^(3,4). This can be summarised by

$$\left. \begin{aligned} N_T &= \frac{D^2}{4L\lambda} = \frac{2M^2}{M-1} N_{eq} \\ R_1 &= \frac{2L}{1-M} \quad R_2 = \frac{2ML}{M-1} \end{aligned} \right] \quad \dots(1)$$

On eliminating M,

$$L = -\frac{1}{2} |R_1| + \frac{1}{4} D \left[\frac{|R_1|}{\lambda N_{eq}} \right]^{\frac{1}{2}} \quad \dots(2)$$

where D = diameter of the rod
 L = cavity length
 M = magnification
 N_{eq} = equivalent Fresnel number which takes values 0.5, 1.5, 2.5
 R_1 = output mirror radius
 R_2 = 100% mirror radius

Equation (2) can be used in the manner described in ref.(2) to calculate the cavity length for a particular output mirror radius. This however could lead to the wrong choice of the magnification M which is the dominant factor determining the stability and efficiency of the system.

In designing the present system the desired output coupling was judged from the performance of a stable oscillator to be between 70% and 80%. Two systems have been designed and operated. For the construction of one of them, eqn. (2) has been used to calculate the length L for a standard mirror radius of -50 cm. The magnification for this system turned out to be 3.54. The other system has been constructed by using the graphs presented by Siegman⁽³⁾ for a required output coupling of 80% giving a magnification of $M = 3.25$. The radii of the mirrors were then calculated from (1) to be $R_1 = 58$ cm and $R_2 = 189$ cm. It was found that the smaller magnification system was more reliable and had a slightly higher efficiency (~ 7%).

In a high repetition rate system the lensing of the laser rod plays a very important part as can be seen from Fig.1. In order to make valid approximations regarding the effective curvature of the back reflector as a combination of the lens in the rod and the radius of the mirror, the latter was placed as near as possible to the rod, with the Pockels cell placed between the rod and the exit mirror as shown schematically in Fig.2.

In order to calculate the radius of the back mirror, we bear in mind that the radiation must emerge parallel after traversing the laser rod twice and being reflected off the back mirror once for a round trip of the cavity. The following simple analysis has been used to calculate the effective mirror radius, assuming that the rod behaves like a simple lens. In Fig.3, O is the confocal point. Tracing the radiation from its parallel condition at the exit backward towards the point O the following relations from geometrical optics can be written:

$$\left. \begin{aligned} \frac{1}{f} &= \frac{1}{f_r} + \frac{1}{f_2} - \frac{d}{f_r f_2} \\ d - x &= \frac{fd}{f_2} \end{aligned} \right] \quad \dots(3)$$

$$\left. \begin{aligned} \frac{1}{F} &= \frac{1}{f_r} + \frac{1}{f} - \frac{x}{f_r f} \\ y &= \frac{Fx}{f_r} \end{aligned} \right] \quad \dots(4)$$

$$F + y - x = \ell \quad \dots(5)$$

where

f_1, f_2 are the focal lengths of the two mirrors

f_r is the focal length of the laser rod

f, F are the focal lengths corresponding to the principal planes P_1 and P_2

d distance of the back mirror from the laser rod

ℓ distance of the confocal point from the laser rod

Eliminating f from eqns.(3) and (4) and substituting in (5)

$$\frac{f_r^2 f_2}{2f_r f_2 + f_r^2 - d(f_r + f_2)} + \frac{df_r f_2^2}{[2f_r f_2 + f_r^2 - d(f_r + f_2)](f_2 + f_r)} - \frac{df_2}{f_2 + f_r} = \ell \quad \dots(6)$$

Note that for $d=0$ this equation reduces to the approximation $\frac{1}{f_r} = \frac{1}{R_2} - \frac{1}{R'_2}$ as described by Herbst et al.⁽²⁾ For $d \ll f_2$ and $d \ll f_r$, equation (6) reduces to

$$\frac{f_r f_2}{2f_2 + f_r} + \frac{df_2^2}{(2f_2 + f_r)(f_2 + f_r)} - \frac{df_2}{f_2 + f_r} = \ell \quad \dots(7)$$

Note that as $f_r \rightarrow \infty$, $\ell \rightarrow f_2$ as expected. Re-arranging eqn.(7) we get

$$f_r^2(f_2 - \ell) + f_r(f_2^2 - df_2 - 3\ell f_2) - df_2^2 - 2f_2^2 \ell = 0 \quad \dots(8)$$

For a specific mirror radius, eqn.(8) can be used to calculate the focal length of the rod f_r and hence, from Fig.1, the pumping of the laser rod for

a collimated output. The output energy of the laser can thus be increased or decreased by changing the back mirror radius to give a parallel beam according to eqn.(8). For $f_2 = \frac{R_2}{2} = 125$ cm, $d = 17.1$ cm and $R_2 = 189$ cm we find that $f_r = 324$ cm. From graph 1 this corresponds to 14J input energy per pulse at 20 pps. Note that there is a great difference from the approximation $\frac{1}{f_r} = \frac{1}{R_2} - \frac{1}{R_2'}$ which, for the above parameters, would give $f_r = 774$ cm. This is due to the fact that no account of the position of the effective mirror was taken in the latter calculation. Note also that the bigger the difference between the effective and actual radius of the mirror becomes the nearer the two calculations come to agree.

One of the important elements of unstable YAG oscillators is the output mirror window. We have constructed a number of output mirrors using optical coatings on anti-reflection coated substrates. Fig.1 shows a curved etalon, anti-reflection coated on both sides, with a 100% reflecting spot at $1.06 \mu\text{m}$ being used as the output mirror. This coating was done by carefully machining metal masks to cover the rest of the area of the substrate. We have also constructed output mirrors on plano-convex substrates followed by plano-concave substrate, to compensate for the resulting lens. Fig.4 shows the reflecting central spot of the output mirror magnified under a high resolution microscope. Its actual size is 1.9 mm. This kind of mirror has the advantages of being much easier to mount and easier to align and they offer the least of technological problems in the construction of their substrates.

EXPERIMENTAL RESULTS

Three systems have been constructed and operated according to the above design, bearing the following parameters:

(1)	(2)	(3)
$2a_1 = 1.8$ mm	$2a_1 = 1.9$ mm	$2a_1 = 1.9$ mm
$D = 6.3$ mm	$D = 6.3$ mm	$D = 6.3$ mm
$R_1 = -50.0$ cm	$R_1 = -58.0$ cm	$R_1 = -58.0$ cm
$R_2' = 176.0$ cm	$R_2' = 203.0$ cm	$R_2' = 250.0$ cm
$L = 63.2$ cm	$L = 65.5$ cm	$L = 65.5$ cm
$d = 15.1$ cm	$d = 17.1$ cm	$d = 17.1$ cm
$M = 3.52$	$M = 3.25$	$M = 3.25$

Systems (2) and (3) were more efficient (approximately 7%) and more reliable than system (1). System (3) produced well over 200 mJ in a collimated beam but it could not be run for long because high pumping caused heating of the recirculating liquid which was not supplied with a heat exchanger. System (2) gave up to 200 mJ in pulses of approximately 10 ns.

Fig.5 shows the input-output curve of a Q-switched unstable Nd:YAG oscillator at 20 pps for a 6.3 mm diameter rod and a magnification of 3.25. Near threshold the line curves slightly in the same way as that expected from a stable resonator. The overall efficiency of the system is 1.2% for pulses of approximately 10 ns.

The output of the free running oscillator was focused on thin metal sheets up to 0.75 mm thick. Figs.6(c,d) show some of the holes drilled in brass and they indicate the uniformity of the beam of the free running oscillator. Other metals such as copper and aluminium were used but although as clear a circular hole could be obtained at the entrance, the holes were filled with wall depositions due to the irregularity of the pulses in time.⁽⁵⁾ Fig.6(a) shows typical polaroid burn patterns of the free running oscillator at the exit mirror. Fig.6(b) shows typical burn patterns of the free running oscillator as it is focused down by a long focal length lens with $f = 128$ cm. No attempt to elaborate on the drilling of materials was made, but the focusing on metal and plastic targets gave us a fair indication of the quality of the beam.

The output beam from the Q-switched oscillator was reflected twice across the room up to a distance of 10m from the exit mirror. Fig.7 shows beam burn patterns on polaroid film at distances of 0.4m, 1m, 2.75m and 8.5m from the exit mirror of the oscillator. In the near field the Fresnel diffraction rings are clearly visible. In the far field most of the energy of the beam was concentrated into a central Gaussian shape pulse with a weak ring round it. Analysis of the beam profile in the near and far fields was done with a scanning diode array. Fig.8(b) shows the intensity distribution of the pulse at a distance of approximately 25 cm. The diameter of the beam at maximum intensity is approximately 4 mm. In the centre the Arago spot is just discernible. Fig.8(c) shows the intensity distribution of the beam at a distance of 9.5m. This is very close to Gaussian with a spot size at the $1/e^2$ point of 2.3 mm

which gives a beam divergence of approximately 0.25 mrad. It is important to point out here that if the confocal condition is not accurately satisfied and the beam is slightly diverging, perfectly symmetric burn patterns can be obtained on polaroid film in the near field. This is due to diffraction at the circumference of the laser rod and it indicates that the beam is not collimated. The best way to check the collimation of the beam is to investigate the beam in the far field or to drive nonlinear devices and note the acceptance angle.⁽²⁾

Fig.8(a) shows the reproducibility of the pulses in time, where 20 superimposed pulses have been recorded using a fast photodiode. The small dip at the end of the pulse is due to a reflection at the cable. Finally the Q-switched output of the laser was focused to form a spark in air with a 20 cm focal length lens. A stationary spark was formed whose position remained constant to better than ± 0.5 mm indicating the reproducibility of the power and divergence of the pulse.

We are at present engaged in the construction of systems with slightly smaller magnification, of around 3. These will be tried on systems whose recirculating cooling liquid would be maintained at constant temperature through a thermostat and a heat exchanger. In this way we hope to try systems with repetition rates of up to 40 pps. We are also preparing masks for the construction of even better quality output mirrors.

The high energy and high efficiency of the unstable resonator in a uni-phase output make it an extremely attractive device in machining applications as well as driving non-linear experiments.

ACKNOWLEDGEMENTS

The author would like to thank Mr. K. Fletcher for the preparation of all the specialised coatings in this paper, Mr. D. De Jong for his assistance during the early phases of the experiments and Dr. I.J. Spalding for his interest in this work.

REFERENCES

1. EWANIZKY, T.F. and CRAIG, J.M. - Applied Optics Vol.15, No.6, pp.1465-1469 (1976)
2. HERBST, R.L., KOMINE, H. and BYER, R.L. - Optics Communications Vol.21, No.1, pp.5-7 (1977)
3. SIEGMAN, A.E. - Laser Focus, pp.42-47, May 1971.
4. SIEGMAN, A.E. - IEEE J.Quantum Electronics QE-12, No.1, pp.35-39 (1976)
5. HERZINGER, G., STEMME, R. and WEBER, H. - IEEE J.Quantum Electronics QE-10, pp.175-178 (1974)

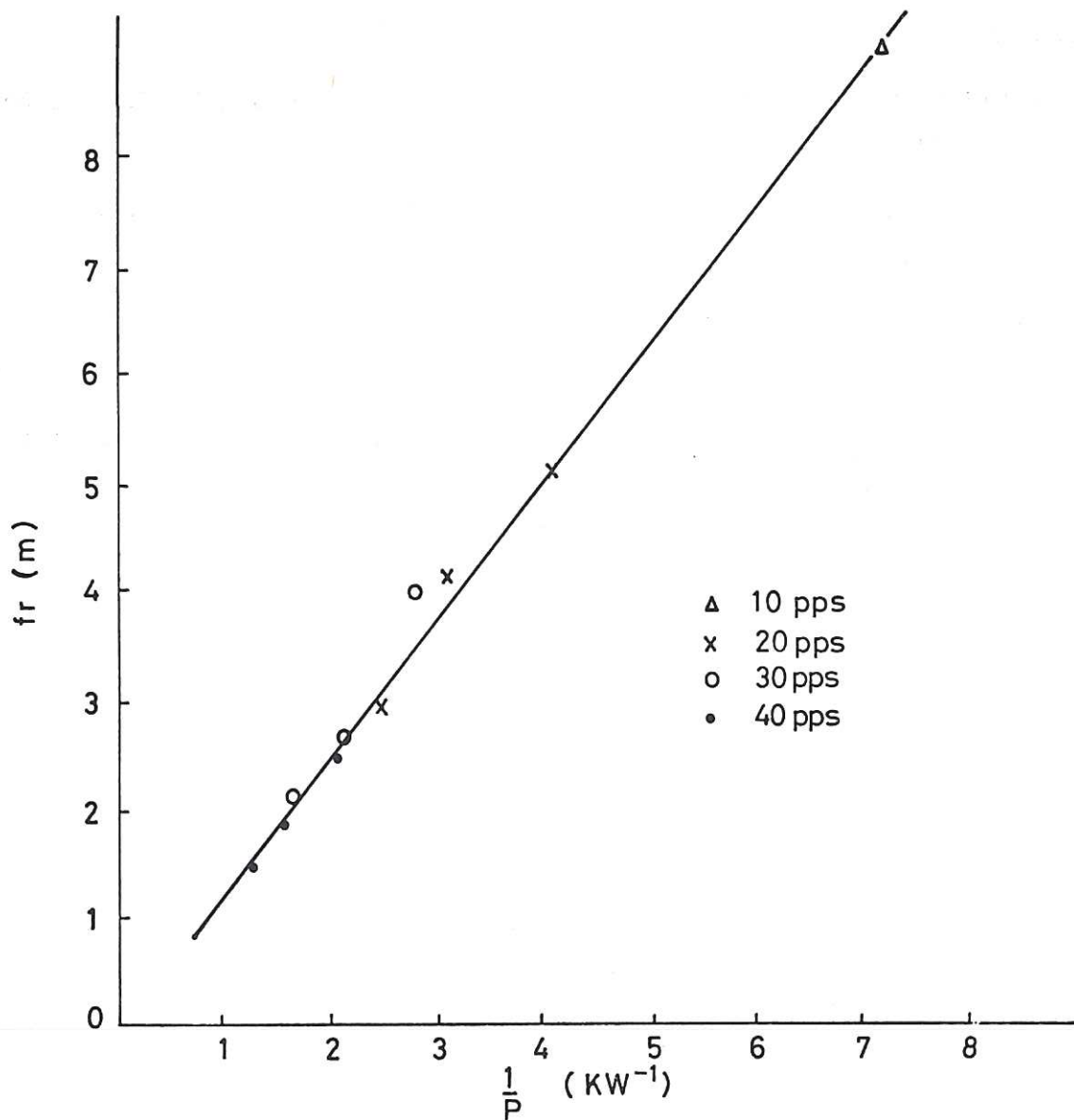


Fig.1 The focal length of the laser rod in metres as a function of the inverse of the input power to the flashlamp in kW^{-1} .

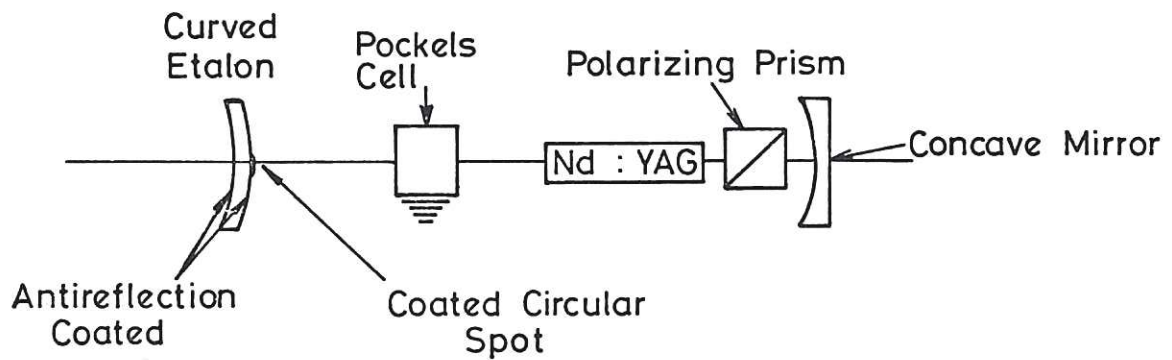


Fig.2 Schematic arrangement of the Q-switched positive branch unstable Nd:YAG oscillator.

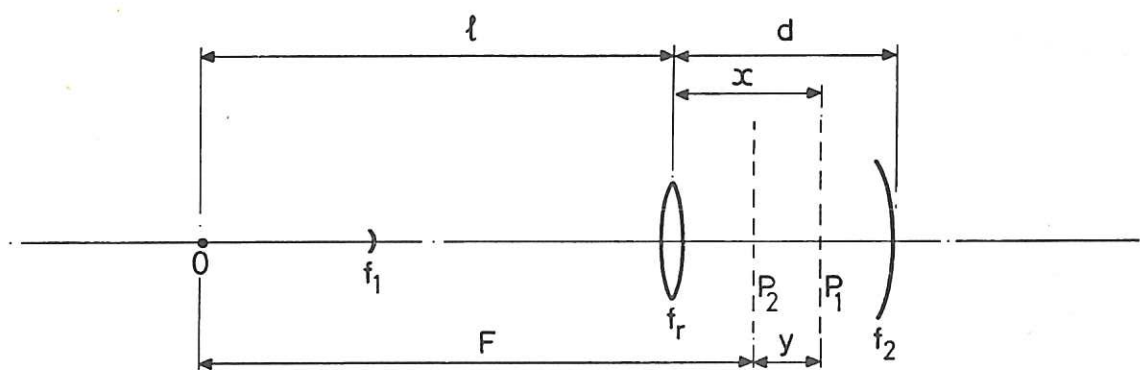


Fig.3 Diagram showing the parameters of the unstable Nd:YAG oscillator for the calculation of the confocal condition. The laser rod is approximated to a thin lens.

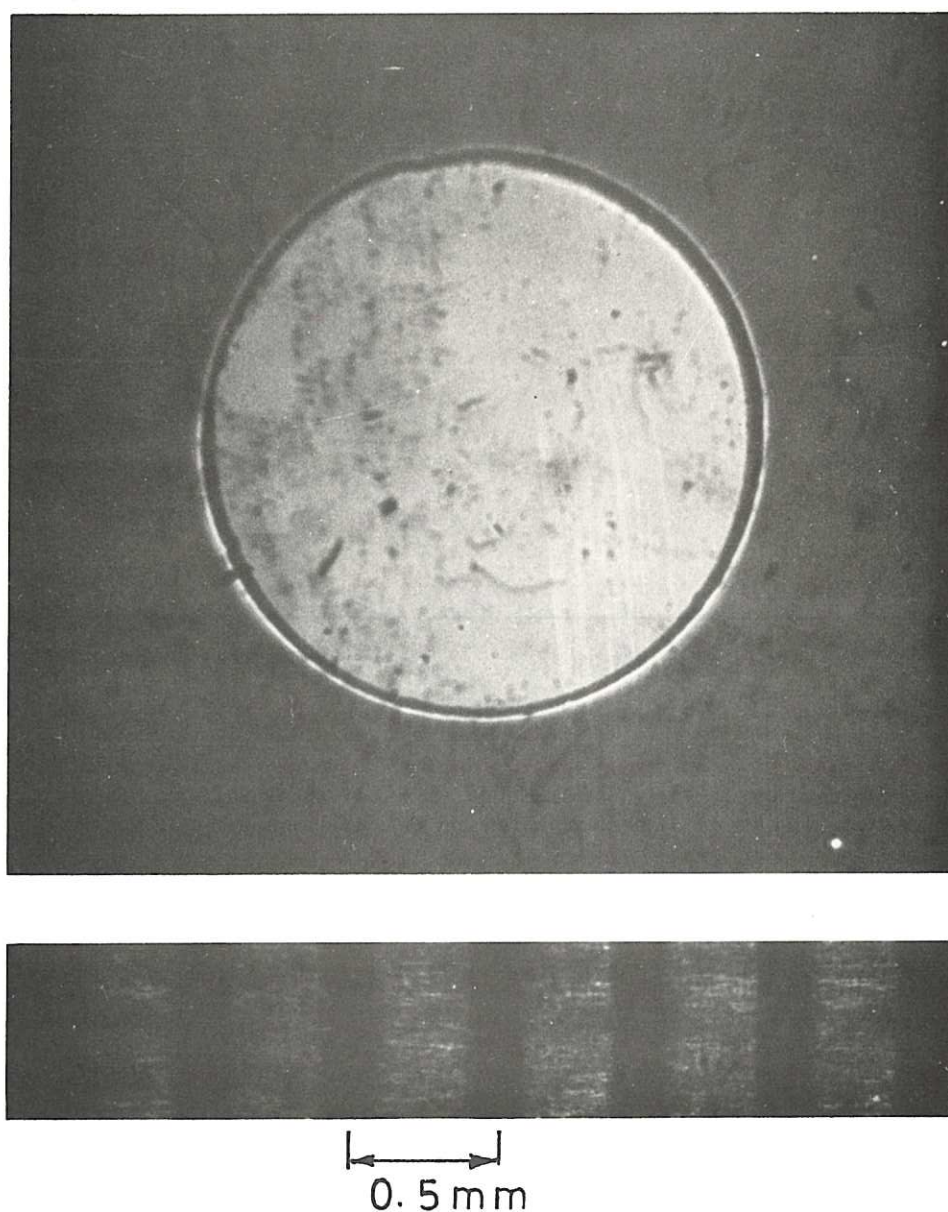


Fig.4 The coating on the output mirror window as seen through a microscope. The actual size is 1.9 mm.

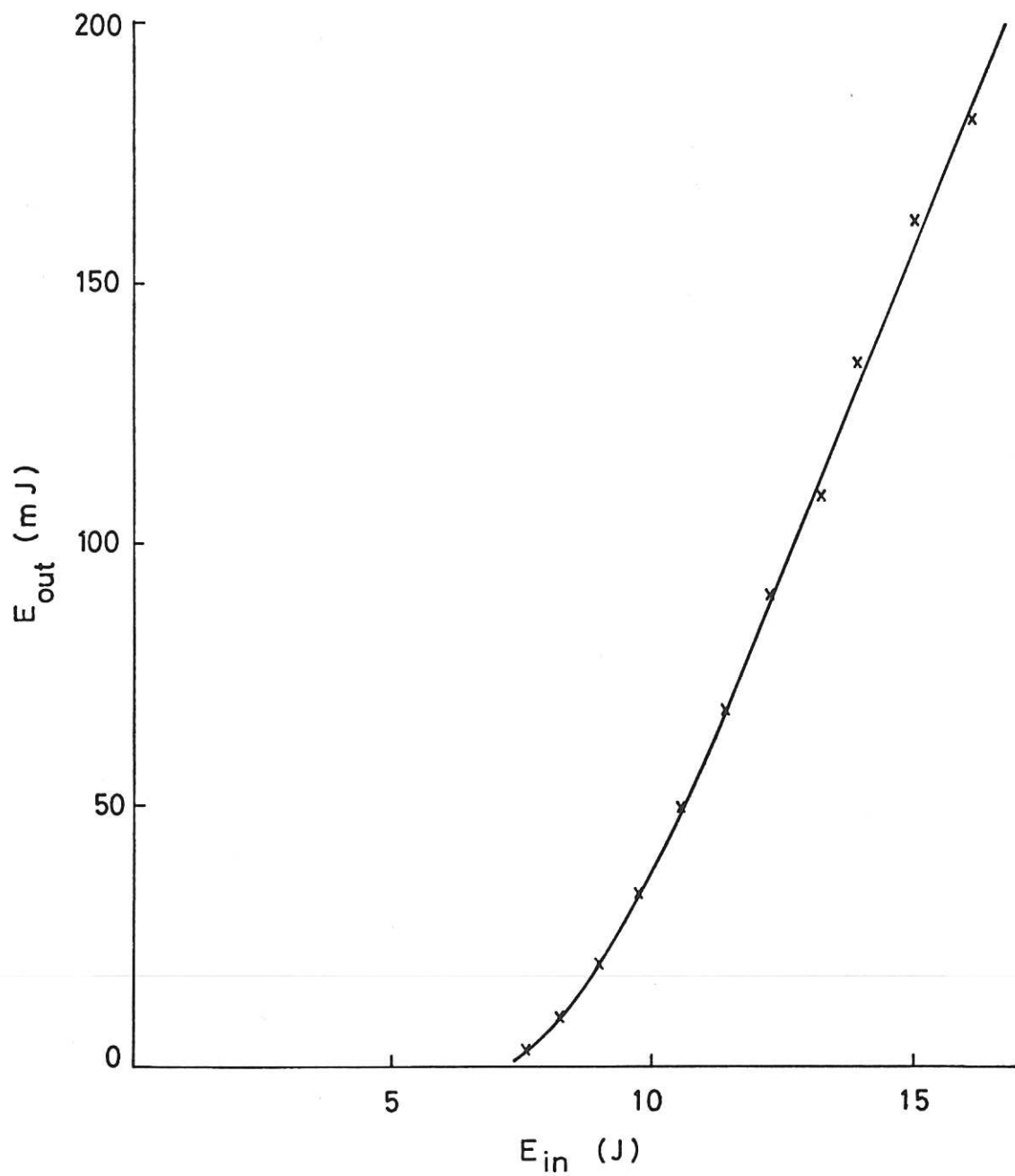
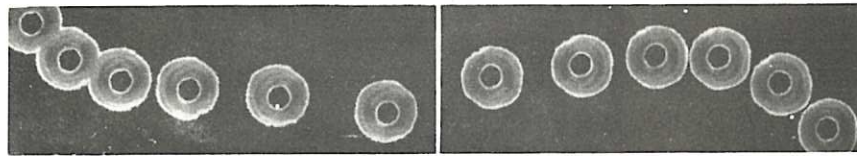
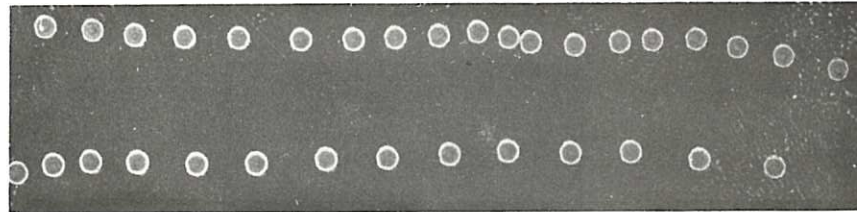


Fig.5 The Q-switched output energy of the unstable Nd:YAG oscillator at 20pps, as a function of input energy to the flashlamp, for a 6.3mm diameter rod and a magnification of $M = 3.25$.



(a) Beam burn patterns from the free running oscillator at the exit mirror.

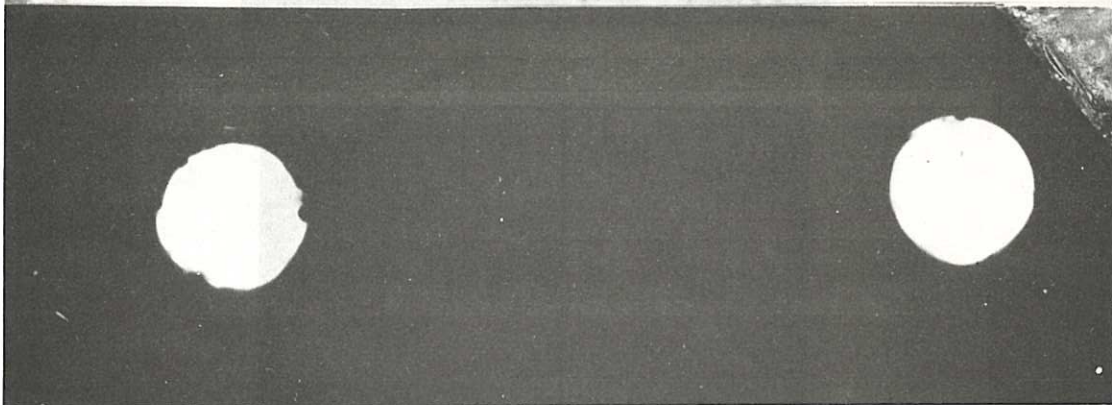


(b) Beam burn patterns from the free running oscillator as it is focused down by a 128 cm focal length lens.

(c)



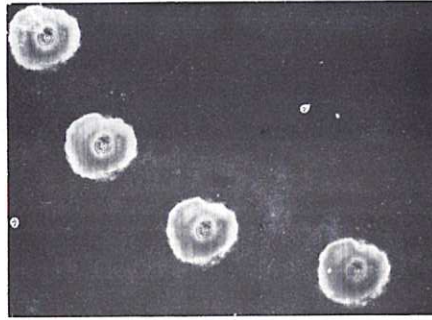
(d)



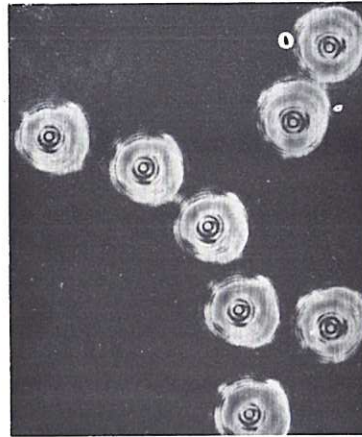
(c) Holes drilled in a brass sheet 0.35 mm thick using the output from the free running unstable resonator as viewed from the top through a microscope.

(d) The same holes as in (c) as viewed through a microscope with the light coming through the holes.

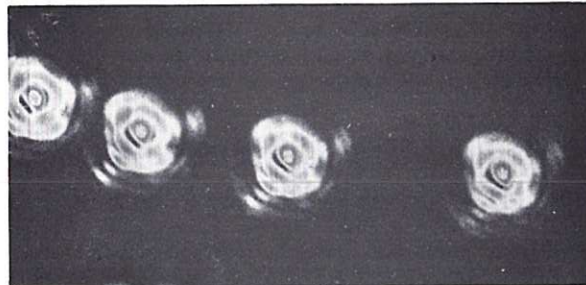
(a)



(b)



(c)



(d)

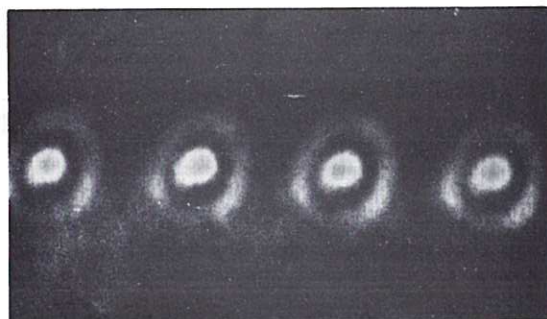
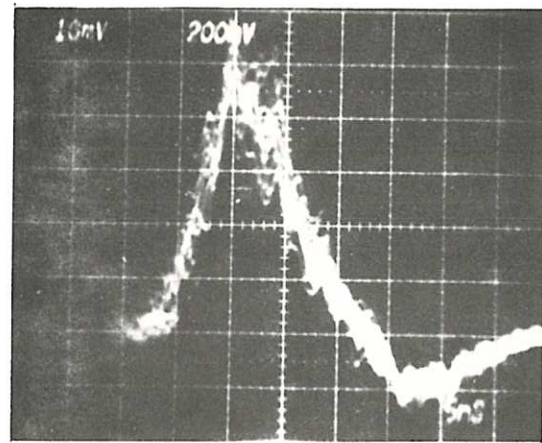


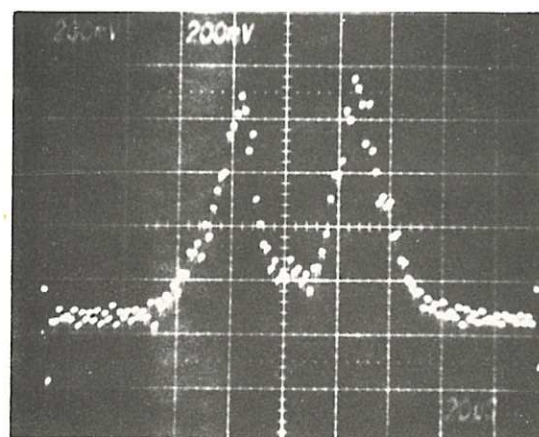
Fig.7 Beam burn patterns on polaroid film obtained from Q-switched oscillator at (a) 0.4m, (b) 1 m, (c) 2.75m and (d) 9.0m from the exit mirror. The Fresnel diffraction rings in the near field are clearly visible.

Figure 8

(a) 20 superimposed Q-switched pulses from the unstable oscillator obtained using a fast photodiode. Output energy 180 mJ; time scale 5 ns/div. The small dip at the end of the traces is due to a reflection in the cable.



(b) The beam profile of the Q-switched output from the unstable resonator at a distance of 25 cm from the exit mirror obtained using a scanning diode array. Time scale 20 μ s/div; 1 μ s = 0.1 mm in space. The Arago spot is discernable in the middle. Diameter of the beam at peak intensity \sim 4 mm.



(c) The beam profile of the Q-switched output from the unstable oscillator at a distance of 9.5 m. Time scale 20 μ s/div; 1 μ s = 0.1 mm in space. Spot size at the $1/e^2$ intensity point \sim 2.3 mm.

